Sample	$^{20}Ne/^{22}Ne$	$^{20}Ne/^{21}Ne$	Remarks
Pure Neon (Linde)	9.800 ± 0.030	339.0 ± 2.0	
Air Neon A	9.795 ± 0.035	337.5 ± 2.5	[b]
Air Neon B	9.800 ± 0.035	338.0 ± 1.5	[a]
Air Neon C	9.795 ± 0.050	—	[b]
Pure Neon (Linde)	—	338.5 ± 2.0	[c]

[a] Prepared from air according to procedure a).
[b] Prepared from air according to procedure b).
[c] Measured on Atlas CH4 mass spectrometer.

Table 1. Isotopic composition of different air neon samples. The errors are three times standard error. The values are corrected for mass discrimination, but the error does not include the uncertainty of our isotopic neon standard.

	$^{20}Ne/^{22}Ne$	$^{20}Ne/^{21}Ne$	$^{22}Ne/^{21}Ne$
This paper	9.800 ± 0.080	338.0 ± 2.5	34.50 ± 0.30
Nier [1]	10.305 ± 0.045	353.7 ± 0.8	34.32 ± 0.08
Dibeler, Mohler, and Reese [2]	9.83 ± 0.19	323 ± 23	32.9 ± 2.3
Hibbs [3]	9.26 ± 0.01	300 ± 10	32.4 ± 1.1
Vaughan, Williams, and Tate [4]	9.25 ± 0.08	337 ± 20	36.4 ± 2.2

Table 2. Comparison of our results with literature values. The errors are taken from the original publications, and may be defined differently (see original publications). The error of our results includes the uncertainty of our isotopic neon standard.

Table 2 gives a comparison of our results with previous determinations. The $^{20}Ne/^{22}Ne$ and $^{20}Ne/^{21}Ne$ values given by Nier [1] are definitely higher, whereas the $^{22}Ne/^{21}Ne$ ratio agrees quite well with our value. Nier explicitly states, that his neon sample might have been fractionated. If this is indeed true then the good agreement of the $^{22}Ne/^{21}Ne$ ratio would be accidental. In all the other previous determinations the mass spectrometer was not checked for possible discriminations and thus no great significance can be attached to either agreement or disagreement with our results.

The abundance ratios found in our work correspond to percentage abundances of 90.50 ± 0.07, 0.268 ± 0.002 and 9.23 ± 0.07 for ^{20}Ne, ^{21}Ne and ^{22}Ne respectively. With isotopic weights of ^{20}Ne, ^{21}Ne and ^{22}Ne of 19.9924, 20.9939 and 21.9914 respectively ($^{12}C = 12$ scale, König, Mattauch, and Wapstra [5]) one calculates an atomic weight of 20.179 ± 0.002 for neon. This value is in fair agreement with the international value of 20.183 based upon gas density measurements (Baxter and Starkweather [6], see also Cameron and Wichers [7]).

We would like to thank Drs. J. Geiss and A. O. Nier for helpful discussions and Dr. K. Clusius for the enriched ^{22}Ne. This work was supported by Schweizerischer Nationalfonds zur Förderung der wissenschaftlichen Forschung (grant number NF 2648 and NF 3045).

[1] A. O. Nier, Phys. Rev. **79**, 450 [1950].
[2] V. H. Dibeler, F. L. Mohler, and R. M. Reese, J. Res. Nat. Bur. Stand. **38**, 617 [1947].
[3] R. F. Hibbs, Mass Spectrometric Measurements of Natural Isotopic Spectra, Report No. AECU-556 [1949].
[4] A. L. Vaughan, J. H. Williams, and J. T. Tate, Phys. Rev. **46**, 327 [1934].
[5] L. A. König, J. H. E. Mattauch, and A. H. Wapstra, Nucl. Phys. **31**, 18 [1962].
[6] G. P. Baxter and H. W. Starkweather, Proc. Nat. Acad. Sci., Wash. **14**, 50 [1928].
[7] A. E. Cameron and E. Wichers, J. Amer. Chem. Soc. **84**, 4175 [1962].

Mattauch–Herzog Type Mass Spectrograph with Two-Stage Electrostatic Field

Isao Takeshita

Research Laboratory, Wireless Division,
Matsushita Electric Industrial Company,
Kadoma, Osaka, Japan

(Z. Naturforschg. **20 a**, 624—625 [1965]; received 20 January 1965)

Mattauch–Herzog type mass spectrographs for chemical analysis of solid material using a spark ion source are powerful. But one point of disadvantage is the fact that the energy slit cannot control the energy spread (β) independently of beam divergence (α). Therefore, even when the energy slit is narrowed to an infinitesimal width, the ion beam which enters the magnetic field still has a wide energy spread.

If two electrostatic fields are substituted for the usual single electrostatic field, a real image of the ion source being formed between the two fields and the energy defining slit being set there, then the energy spread can be controlled independently of beam divergence.

If the electrostatic fields are produced by cylindrical condensers with equal radii as shown in Fig. 1, then the positions of source and image with respect to the electrostatic fields, under the first-order double focusing condition for all masses, are given by the following equations

$$\frac{l_1}{r_e} = \frac{(1/\sqrt{2})\, D_3 \cos\sqrt{2}\,\varphi_{e1} + \sin\sqrt{2}\,\varphi_{e2}\{1-(1\mp 1)\cos\sqrt{2}\,\varphi_{e1}\}}{\{D_3 - \sqrt{2}(1\mp 1)\sin\sqrt{2}\,\varphi_{e2}\}\sin\sqrt{2}\,\varphi_{e1}},$$

$$\frac{l_2}{r_e} = \frac{D_3 - \sqrt{2}\sin\sqrt{2}\,\varphi_{e2}(1\mp 1-\cos\sqrt{2}\,\varphi_{e1})}{2\sin\sqrt{2}\,\varphi_{e1}\sin\sqrt{2}\,\varphi_{e2}}, \quad \frac{l_3}{r_e} = \frac{1}{\sqrt{2}}\cot\sqrt{2}\,\varphi_{e2}.$$

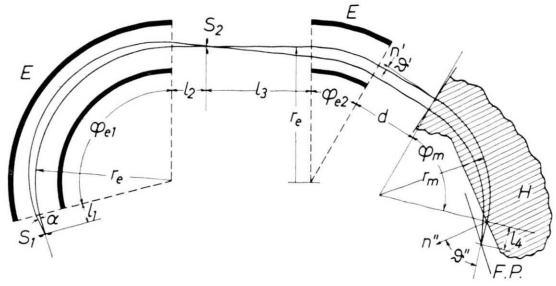

Fig. 1. MATTAUCH–HERZOG type mass spectrograph with two-stage electrostatic field. E electrostatic field; H homogeneous magnetic field; S_1 source slit; S_2 energy slit; F.P. focal plane.

The coordinates used and the significance of the quantities l_1, l_2, l_3, φ_{e1}, φ_{e2} etc. are illustrated in Fig. 1. D_3 is a constant which characterizes the magnetic field. It has the form $\mu_{1b}\,\nu_{2a}-\nu_{1b}\,\mu_{2a}$ using HINTENBERGER's notation [1]. The upper sign is valid for deflections in the two electrostatic fields in the same sense and the lower sign for opposite deflections. In the former case, the resolving power (R) is the same as that of the usual MATTAUCH–HERZOG type instrument:

$$R = r_e/2\,s\,,$$

where s is the width of the source slit. In the latter case, it is

$$R = \frac{r_e}{2\,s}\,\frac{D_3}{2\sqrt{2}\sin\sqrt{2}\,\varphi_{e2}-D_3}\,.$$

This implies the possibility of increasing the resolving power.

In the usual MATTAUCH–HERZOG type mass spectrograph the ion beams entering the magnetic field cannot be parallel in the second-order approximation, but in our type they can. If the two-stage electrostatic field is followed by a homogeneous magnetic field characterized by $D_4=\mu_{1b}\,\nu_{11c}-\nu_{1b}\,\mu_{11c}=0$, this results in a special MATTAUCH–HERZOG type mass spectrograph in which the second-order angular aberration becomes zero for all points on the first-order focal plane.

In addition to these fine characters, the coefficient for the mixed velocity- and angle-dependent aberration becomes zero at the point on the focal plane which corresponds to the magnetic radius r_{m0}, and the coefficient for the second-order velocity aberration can be made to vanish at the same point by a particular choice for d/r_e.

Table 1 gives examples of such mass spectrographs which provide first-order double focusing and α^2 focusing for all masses and $\alpha\beta$ and β^2 focusing for one mass.

The coefficients T_{18} and T_{19} of the $\alpha\beta$ and β^2 aberrations respectively, are given by

$$T_{18}/r_m = \bar{T}_{18}(1-1/\tau)\,,$$
$$T_{19}/r_m = \bar{T}_{19}(1-1/\tau)\,,$$

where $\tau = r_m/r_{m0}$.

The numerical values of $\bar{T}_{18}$ and $\bar{T}_{19}$ are given in the last two columns of Table 1, showing that the $\alpha\beta$ and β^2 aberrations are also small in a wide range.

[1] H. HINTENBERGER and L. A. KÖNIG, Z. Naturforschg. **12 a**, 140 [1957].

D_3	φ_m	ϑ'	ϑ''	φ_{e1}	φ_{e2}	l_1/r_e	l_2/r_e	l_3/r_e	l_4/r_m	r_{m0}/r_e	d/r_e	T_{18}	$\bar{T}_{19}$
1.0	73° 08′	3° 28′	−53° 26′	112° 49′	33°	0.186	0.0711	0.667	0.247	0.244	0.587	1.429	−2.229
0.9	68° 28′	−2° 44′	−55° 46′	90° 06′	30°	0.403	0.299	0.774	0.227	0.187	0.995	1.915	−3.409
0.8	63° 16′	−9° 37′	−58° 22′	94° 02′	35° 21′	0.650	0.0546	0.593	0.205	0.309	0.232	1.207	−2.167

Table 1. Examples of Mass Spectrographs with corrected α^2 image defect for all masses and corrected β-dependent image defects at one point of the photoplate.

Die Erzeugung intensiver Molekularstrahlen mit Hilfe von Laval-Düsen und ihre Anwendung auf Streuexperimente

E. HUNDHAUSEN und H. PAULY

Institut für Angewandte Physik der Universität Bonn

(Z. Naturforschg. **20 a**, 625—627 [1965]; eingegangen am 5. März 1965)

Die maximale Strahldichte, die sich mit Hilfe einer üblichen Molekularstrahlquelle am Ort des Detektors erreichen läßt, ist durch die sog. „Ofenbedingung" bestimmt. Für einen Strahlweg von der Länge 1 m läßt sich ein „Standard-Strahl" definieren [1], dessen Dichte

$$N = 5\cdot 10^{10}\ \text{Moleküle/sec mm}^2$$

im allgemeinen mit keinem Molekularstrahlofen wesentlich überschritten werden kann [2].

Die Intensität dieses Standard-Strahles reicht jedoch für viele Untersuchungen auch dann nicht aus, wenn ein Detektor großer Nachweisempfindlichkeit benutzt werden kann. Beispiele hierfür sind Messungen des differentiellen Streuquerschnittes im Bereich großer Winkel für elastische und unelastische Stöße zwischen neutralen Molekülen, wo die zu messende Streuintensität (unter Berücksichtigung von Winkelauflösung, Geschwindigkeits- und Zustandsselektion) um einen Faktor 10^5 bis 10^9 kleiner sein kann als die Intensität des einfallenden Strahles.

Wesentlich höhere Strahlintensitäten lassen sich unter Verwendung von LAVAL-Düsen erzielen [3–5]. Bisher scheinen nur Untersuchungen an Gasen vorzuliegen, für die sehr aufwendige Apparaturen hoher Saugleistung benötigt werden. Dieser Nachteil wird bei der Verwendung leicht kondensierbarer Dämpfe vermieden.

[1] H. G. BENNEWITZ u. R. WEDEMEYER, Z. Phys. **172**, 1 [1963].
[2] G. BECKER, Z. Angew. Phys. **13**, 59 [1961]; Z. Phys. **162**, 290 [1961].
[3] A. KANTROWITZ u. J. GREY, Rev. Sci. Instrum. **22**, 328 [1951].
[4] E. W. BECKER u. W. HENKES, Z. Phys. **146**, 320 [1956].
[5] J. DECKERS u. J. B. FENN, Rev. Sci. Instrum. **34**, 96 [1963].